Mean-field analysis in the *p-d* model of oxide superconductors

S. Ishihara, H. Matsumoto, S. Odashima, and M. Tachiki
Institute for Materials Research, Tohoku University, Sendai 980, Japan

F. Mancini
Dipartimento di Fisica Teorica SMSA, Universitá di Salerno, 84140 Baronissi(SA), Italy
(Received 30 March 1993)

A highly correlated *p-d* model of cuprate oxide superconductors is analyzed by use of composite operators on CuO_2 clusters. A minimal set of composite operators to describe the electronic state is identified from the criterion that the order of the approximation is determined by coupling constants multiplied by the weight of their respective operators. It is shown that the intensity transfer among bands with hole doping is well described within the mean-field approximation. Effects of the nearest-neighbor spin correlation are investigated and it is shown that the band dispersions are strongly affected. By the local antiferromagnetic correlation, the band dispersion of the upper Hubbard band is flattened in the whole Brillouin zone, while that of the *p* dominant band near the Fermi level is flattened only around a certain region centered at the zone boundary. In the moderately doped region, the Fermi surface is consistent with a large Fermi surface.

I. INTRODUCTION

Since the discovery of the high-T_c superconductors, the electronic structure of CuO_2 planes has been investigated intensively in order to understand the speciality of electronic properties in oxide cuprate superconductors. From experimental and theoretical analyses, the following facts have been usually accepted: The parent insulator is a charge-transfer insulator whose gap is formed between the upper Hubbard level of Cu $d_{x^2-y^2}$ orbitals and O p_x and O p_y orbitals.[1,2] A highly correlated *p-d* model is suitable to describe the electronic state of oxide cuprate superconductors.[3–5] The doping dependence of the electronic state is not rigid-band-like, but an intensity transfer from the high-energy region to the low-energy region is induced.[6–9] This shift of the intensity occurs without collapsing the level distances. With hole doping a highly correlated in-gap band is formed[10–12] and it has a large Fermi surface.[13–16] In a heavily doped region, the electronic structure is more bandlike and the system behaves as a normal metal. There are many theoretical works investigating the nature of the electronic state in oxide superconductors by use of the *p-d* model.[17–27] It has been argued that the model may be reduced to a simple Hubbard model,[28,29] *t-J* model,[30] or Heisenberg-Kondo model.[31–33] The electronic state near the Fermi level in the moderately doped region is still controversial in a conventional Fermi liquid state,[21,28,29,34] resonating-valence-bond state,[35,36] Luttinger-liquid state,[37] and marginal Fermi-liquid state.[38]

In previous papers[22] we have proposed to describe the electronic excitations as combinations of composite electronic excitations on CuO_2 clusters. Strong correlation may create certain excitation modes extended over several lattice points in which several modes are simultaneously excited. By considering certain combinations of composite operators extended over several lattice points, one can extract the desired excitation modes. Then the propagation of electronic excitations is described as a repetition of those composite excitations. We have shown that the change of electronic states near the metal-insulator transition is understood from the level shift and mixing among composite excitations and also have pointed out the possible description of the crossover from a correlated band to a simple bandlike structure. A similar approach may be found in Refs. 23 and 24.

There are several reasons to revisit the mean-field analysis of the electronic state in the *p-d* model by the composite-operator method. The first reason is to see whether or not there is a better choice of operators which reproduces the result of Ref. 22 more easily in the mean-field level. This means that we look for a better combination of operators to describe quasiparticle excitations. In Ref. 22 the transfer of intensity shows qualitatively correct behavior after the inclusion of the dynamical correction in the self-energy. However, the self-energy used there still has a large component in the high-energy region, which prevents a further detailed investigation of the low-energy behavior. The fact that there is a large high-energy component in the self-energy may indicate that an additional composite operator is necessary to take care of its contribution. Then we ask the general question of how to determine a better choice of composite operators and how to estimate the order of approximation which determines the distribution of the main weight. In this paper we will find a general rule to identify an expansion series of composite operators to describe a highly correlated electron system. It will be shown that expansion parameters are coupling constants multiplied by the weight of operators. We will demonstrate that the operator series chosen according to the obtained criterion improves the approximation very much, by comparing the result of approximate calculations and the exact result for the single-cluster case. The second reason is to clarify what factors control the distribution of the main

weight in the p-d model. In the mean-field approximation treated in this paper, the on-site property is described quite well, as will be shown in the single-cluster analysis. As for intersite contributions, the present mean-field approximation takes care of up to the tb order according to the estimation of the operator weight, where t is the p-d mixing energy and b is a p-d mixing parameter which is proportional to t/Δ (Δ is the charge-transfer gap) for small t/Δ. The correction beyond the mean-field approximation is of the tb^3 order. This indicates that it is now possible to investigate quantities which play sensitive roles to change the distribution of the density of states in the energy scale of tb. In the previous paper, the nearest-neighbor spin-correlation effect is neglected. Such an effect is expected to affect band dispersions through the Pauli principle. Simplification of the calculation due to the mean-field approximation enables us to investigate the effect of the nearest-neighbor spin correlation to the density of states. It will be shown that the nearest-neighbor antiferromagnetic correlation works to narrow the bandwidth of the upper Hubbard band, while the p-dominant band near the Fermi level is narrowed only around a certain region centered at the zone boundary. In the moderately doped region, the results are consistent with a large Fermi surface. It will be pointed out that the flattening of the p band occurs within the energy region of the tb^3 order.

The paper is organized as follows. In the next section, the formula for the p-d model in the composite-operator method is presented. In Appendix A, the composite-operator method presented in Ref. 22 is summarized in an elaborated form, and in Appendix B, explicit forms of mean fields are presented. There the operator expansion is fully used and the mean fields are expressed in a compact form by use of expansion coefficients. In Sec. III the results of numerical calculations are presented. First the approximation method is applied to the single-cluster case and the result is compared with the exact one. For a wide range of parameters, both results coincide quite well. By including intersite effects, the change of the band structure with hole doping is investigated. We show that the present mean-field result produces a doping dependence of the electronic state similar to the one in Ref. 22. In addition, the effect of the nearest-neighbor spin correlation is investigated and it is shown that, by the nearest-neighbor antiferromagnetic correlation, the upper Hubbard band is flattened, while the p band near the Fermi level is flattened only around a certain region centered at the zone boundary. A possible relation to the t-J model is discussed. Section V is devoted to concluding remarks, and in Appendix C the exact result of the single-site case is presented.

II. p-d MODEL

Let us consider the highly correlated p-d model used in Ref. 22. Starting from the tight-binding model composed of d electrons in Cu $d_{x^2-y^2}$ orbitals and p electrons in O p_x, p_y orbitals on a CuO_2 plane, taking only the transition to the upper Hubbard level (Cu $d^9 \leftrightarrow$ Cu d^{10} transition), and considering only bonding p electrons, we have

$$H=\int dx \sum_{\sigma} \{\tfrac{1}{2}\varepsilon_\eta \eta_\sigma^\dagger(x)\eta_\sigma(x)+\varepsilon_p p_\sigma^\dagger(x)p_\sigma(x) +2t[\eta_\sigma^\dagger(x)p_{\sigma\gamma}(x)+p_{\sigma\gamma}^\dagger(x)\eta_\sigma(x)]\} , \tag{2.1}$$

where ε_p and ε_η are bare energies of the p-electron level and upper Hubbard level measured from the Fermi level, respectively, and

$$\eta_\sigma(x)=d_\sigma(x)n_{-\sigma}(x) , \tag{2.2}$$

$$n_{-\sigma}(x)=d_{-\sigma}^\dagger(x)d_{-\sigma}(x) , \tag{2.3}$$

$$p_{\sigma\gamma}(x)=\gamma(-i\nabla)p_\sigma(x) , \tag{2.4}$$

and

$$\gamma(\mathbf{k})^2=1+\gamma_1(\mathbf{k}) , \tag{2.5a}$$

with

$$\gamma_1(\mathbf{k})=-\tfrac{1}{2}(\cos k_x a+\cos k_y a) , \tag{2.5b}$$

where a is the lattice constant. Hereafter we use spinor notation and drop the index showing the spin freedom of electrons unless it is necessary.

In the composite-operator method presented in Ref. 22, electronic excitations are expressed by identifying a certain series of electron operators ψ_n. A summary of the method is presented in Appendix A. The retarded function $\langle R\psi_n(x)\psi_l^\dagger(y)\rangle$ is obtained in the form

$$\mathcal{F}\langle R\psi_n(x)\psi_l^\dagger(y)\rangle = \left[\frac{1}{\omega-[m(\mathbf{k})+\delta m(\omega,\mathbf{k})]I(\mathbf{k})^{-1}}I(\mathbf{k})\right]_{nl} , \tag{2.6}$$

where $\mathcal{F}$ indicates the Fourier transform (see Appendix A). The normalization $I(\mathbf{k})$ and the mean field $m(\mathbf{k})$ are determined from

$$(I(\mathbf{k}))_{nl}=\mathcal{F}\langle\{\psi_n(\mathbf{x}),\psi_l^\dagger(\mathbf{y})\}\rangle \tag{2.7}$$

and

$$(m(\mathbf{k}))_{nl}=\mathcal{F}\left\langle\left\{i\frac{\partial}{\partial t}\psi_n(\mathbf{x}),\psi_l^\dagger(\mathbf{y})\right\}\right\rangle , \tag{2.8}$$

and $\delta m(\omega,\mathbf{k})$ indicates the dynamical correction. The neglect of $\delta m(\omega,\mathbf{k})$ defines the mean-field approximation.

In previous papers we have chosen as a series of fermionic operators p, η, and $p_\gamma\delta n_\mu$ ($\equiv p_\mu$) with $\delta n_\mu=d^\dagger\sigma_\mu d-\langle d^\dagger\sigma_\mu d\rangle$ ($\sigma_\mu=1$ for $\mu=0$ and σ_i for $\mu=1,2,3$). There the mean-field result and the result with a dynamical correction show a drastic difference due to the large contributions from the high-energy parts in the self-energy. This indicates that the choice of the series is not enough to handle the high-energy part in the mean-field level. In fact, we can see that the operator $p_\gamma\eta^\dagger\sigma_i p_\gamma$ has weight of the order of 1, and it mixes directly with $p_\gamma\delta n_i$, which has a dominant contribution near the Fermi level.

In order to remedy the mean-field result in Ref. 22, we use the following criterion in order to identify an opera-

tor series $\psi_n(x)$. As is in Ref. 22, the operators should appear in the successive use of the equations of motion obtained from the fundamental fields $p(x)$ and $\eta(x)$. Independent components are identified from the operator products of fundamental operators, since the primal energies of local excitations are given by the sum of the energies of the constituent operators. Differently from Ref. 22, we choose only operators which have a nonsmall weight. One may think that, in order to express the electronic state near the Fermi level, it is enough to choose operators relating to excitations around the Fermi level. This is not true because the relative energy positions of composite operators before mixing change the intensity distribution, and the energy positions are affected by operators directly mixed with them; that is, when there is an operator which directly mixes with operators situated near the Fermi level and which has a nonsmall weight, one should include it as a member of the operator series in this scheme.

To treat contributions from operators with small weight I as perturbation is also important in the present scheme for the following reason. When I is small, the error for mI^{-1} is large. For example, the energy shift arising from the mixing expressed as $[H,\psi_0]=t\psi_1$ is roughly $\pm t^2 I_1/I_0(\varepsilon_0-\varepsilon_1)$ with I_0,I_1 and $\varepsilon_0,\varepsilon_1$ being the weight and zeroth energy of ψ_0,ψ_1, respectively. When I_1 is small and the level shift is evaluated from $m_{11}I_1^{-1}$, one needs accuracy of I_1^2 order for the evaluation of m_{11}, which becomes an origin of inaccuracy in the approximate calculation. Therefore the contribution from operators with small weight should be treated as a perturbation in the dynamical correction.

According to the above consideration, we have arrived as the choice of electron operators, p-electron operator $p(x)$, restricted d-electron operator $\eta(x)$, p-electron operator with Cu spin flip $p_s(x)$ $[=\sigma p_\gamma(x)\mathbf{n}(x)]$, and p-electron operator with p-d charge transfer $\phi(x)$ $[=-\sqrt{2/n}\,\eta^\dagger(x)\cdot p_\gamma(x)p_\gamma(x)]$. We denote these four components by orthogonalizing as follows:

$$\begin{pmatrix}\psi_1\\ \psi_2\\ \psi_3\\ \psi_4\end{pmatrix}=\begin{pmatrix}p\\ r\\ P\\ \Phi\end{pmatrix}=\begin{pmatrix}p\\ (\sqrt{2/n})\eta\\ p_s-3br\\ \phi-bp_\gamma-c_\phi P\end{pmatrix}, \tag{2.9}$$

where we use the notations

$$p_s=\sigma p_\gamma\mathbf{n},\quad \phi=-r^\dagger\cdot p_\gamma p_\gamma\ . \tag{2.10}$$

The coefficients b and c_ϕ are chosen to satisfy the orthogonality

$$\langle\{P,p^\dagger\}\rangle=\langle\{P,r^\dagger\}\rangle=0\ , \tag{2.11a}$$

$$\langle\{\Phi,p^\dagger\}\rangle=\langle\{\Phi,r^\dagger\}\rangle=\langle\{\Phi,P^\dagger\}\rangle=0\ , \tag{2.11b}$$

and we have

$$b=\langle p_\gamma r^\dagger\rangle\ , \tag{2.12}$$

$$c_\phi=\langle\{\phi,P^\dagger\}\rangle(I_P)^{-1}\ , \tag{2.13}$$

with

$$I_P=\langle\{P,P^\dagger\}\rangle\ . \tag{2.14}$$

Denoting the normalization of Φ as I_Φ,

$$I_\Phi=\langle\{\Phi,\Phi^\dagger\}\rangle\ , \tag{2.15}$$

we have the normalization matrix I_{nm} in the form

$$I=\begin{pmatrix}1&0&0&0\\ 0&1&0&0\\ 0&0&I_P&0\\ 0&0&0&I_\Phi\end{pmatrix}. \tag{2.16}$$

Explicit forms of I_P and I_Φ are summarized in Appendix B. The equations of motion of ψ_n are obtained from the Heisenberg equations

$$i\frac{\partial}{\partial t}p(x)=\varepsilon_p p(x)+t_n r_\gamma(x)\ , \tag{2.17a}$$

$$i\frac{\partial}{\partial t}r(x)=t_n p_\gamma(x)+\varepsilon_\eta r(x)-\frac{t_n}{n}[p_s(x)-p_0(x)]\ , \tag{2.17b}$$

$$i\frac{\partial}{\partial t}p_s(x)=\varepsilon_p p_s(x)+t_n[3\phi(x)+h_s(x)]\ , \tag{2.17c}$$

$$i\frac{\partial}{\partial t}\phi(x)=-2t_n\frac{n-1}{n}p_\gamma(x)-t_n\frac{2}{n}p_0(x)+(2\varepsilon_p-\varepsilon_\eta)\phi(x)+t_n\psi(x)\ , \tag{2.17d}$$

with

$$t_n=2t\sqrt{n/2}\ , \tag{2.18}$$

$$p_0(x)=p_\gamma(x)\delta n(x)\ , \tag{2.19}$$

$$h_s=\sigma(r_{\gamma_1}\mathbf{n}-p_\gamma p_\gamma^\dagger\sigma r)\ , \tag{2.20}$$

$$\psi=-r^\dagger\cdot p_\gamma r_{\gamma_1}-r^\dagger\cdot r_{\gamma_1}p_\gamma+p_\gamma^\dagger\cdot p_\gamma p_\gamma-\frac{1}{n}p_\gamma^\dagger\sigma^\lambda\delta n_\lambda p_\gamma p_\gamma\ . \tag{2.21}$$

Here use was made of the algebra

$$r_s^\dagger r_\sigma=2\left[1-\frac{1}{n}+\frac{1}{n}\delta n\right]\delta_{\sigma s} \tag{2.22a}$$

and

$$r_\sigma r_s^\dagger=\left[-1+\frac{2}{n}\right]\delta_{\sigma s}-\frac{1}{n}\delta n_\mu(\sigma_\mu)_{\sigma s}\ . \tag{2.22b}$$

From Eqs. (2.17), the mean field $m_{nl}=\langle\{i\partial\psi_n/\partial t,\psi_l^\dagger\}\rangle$ is obtained in the form

$$m=\begin{pmatrix}\varepsilon_p & t_n\gamma(\mathbf{k}) & 0 & 0\\ t_n\gamma(\mathbf{k}) & \varepsilon_r & -\frac{t_n}{n}cI_P & -\frac{t_n}{n}dI_\Phi\\ 0 & -\frac{t_n}{n}cI_P & m_P & m_{P\Phi}\\ 0 & -\frac{t_n}{n}dI_\Phi & m_{\Phi P} & m_\Phi\end{pmatrix}, \tag{2.23}$$

where

$$\varepsilon_r=\varepsilon_\eta-2\frac{t_n}{n}b \ , \tag{2.24}$$

$$cI_P=\langle\{p_s-p_0,P^\dagger\}\rangle \ , \qquad dI_\Phi=\langle\{p_s-p_0,\Phi^\dagger\}\rangle \ , \tag{2.25}$$

$$m_P=\left\langle\left\{i\frac{\partial}{\partial t}P,P^\dagger\right\}\right\rangle \ , \qquad m_{P\Phi}=\left\langle\left\{i\frac{\partial}{\partial t}P,\Phi^\dagger\right\}\right\rangle \ , \tag{2.26}$$

$$m_{\Phi P}=\left\langle\left\{i\frac{\partial}{\partial t}\Phi,P^\dagger\right\}\right\rangle \ , \qquad m_\Phi=\left\langle\left\{i\frac{\partial}{\partial t}\Phi,\Phi^\dagger\right\}\right\rangle \ . \tag{2.27}$$

The explicit forms of c, d, m_P, $m_{P\Phi}$, $m_{\Phi P}$, and m_Φ are presented in Appendix B.

The residual interaction, which induces dynamical corrections, is obtained as

$$\delta j_n=t_n\begin{pmatrix}0\\ \frac{1}{n}\delta p_0\\ \delta h_s\\ \delta\psi\end{pmatrix} , \tag{2.28}$$

$$\delta p_0=p_\gamma\delta n-br-c_0P-d_0\Phi \ , \tag{2.29a}$$

$$\delta h_s=\sigma(r_{\gamma_1}\mathbf{n}-p_\gamma p_\gamma^\dagger\sigma r)-3b_{hs}r-3c_{hs}P-3d_{hs}\Phi \ , \tag{2.29b}$$

$$\delta\psi=-\left[r^\dagger\cdot p_\gamma r_{\gamma_1}+r^\dagger\cdot r_{\gamma_1}p_\gamma-p_\gamma^\dagger\cdot p_\gamma p_\gamma+\frac{1}{n}p_\gamma^\dagger\sigma^\lambda\delta n_\lambda p_\gamma p_\gamma\right]-a_\psi p_\gamma-b_\psi r-c_\psi P-d_\psi\Phi \ . \tag{2.29c}$$

Here we have defined, for an arbitrary operator A, expansion coefficients with respect to ψ_n as

$$A=a_A p_\gamma+b_A r+c_A P+d_A\Phi+\delta A \ , \tag{2.30}$$

where

$$a_A=\langle\{A,p^\dagger\}\rangle\gamma^{-1} \ , \tag{2.31a}$$

$$b_A=\langle\{A,r^\dagger\}\rangle \ , \tag{2.31b}$$

$$c_A=\langle\{A,P^\dagger\}\rangle I_P^{-1} \ , \tag{2.31c}$$

$$d_A=\langle\{A,\Phi^\dagger\}\rangle I_\Phi^{-1} \ , \tag{2.31d}$$

and

$$\langle\{\delta A,\psi_n^\dagger\}\rangle=0 \ . \tag{2.32}$$

The retarded function in the mean-field approximation is obtained from Eq. (2.6) with $\delta m(\omega,\mathbf{k})=0$. For example, we have, for p and r propagators,

$$S_{pp}(\omega,\mathbf{k})=\frac{1}{\omega-\varepsilon_p-t_n^2\gamma^2(\mathbf{k})[\omega-\varepsilon_r-\Sigma_r(\omega,\mathbf{k})]^{-1}} \ , \tag{2.33}$$

$$S_{rr}(\omega,\mathbf{k})=\frac{1}{\omega-\varepsilon_r-\Sigma_r(\omega,\mathbf{k})-t_n^2\gamma^2(\mathbf{k})(\omega-\varepsilon_p)^{-1}} \ , \tag{2.34}$$

with

$$\Sigma_r(\omega,\mathbf{k})=\left[\frac{t_n}{n}\right]^2(c\ d)\begin{bmatrix}\omega-m_P(\mathbf{k})I_P(\mathbf{k})^{-1} & -m_{P\Phi}(\mathbf{k})I_\Phi(\mathbf{k})^{-1}\\ -m_{\Phi P}(\mathbf{k})I_P(\mathbf{k})^{-1} & \omega-m_\Phi(\mathbf{k})I_\Phi(\mathbf{k})^{-1}\end{bmatrix}^{-1}\begin{bmatrix}cI_P(\mathbf{k})\\ dI_\Phi(\mathbf{k})\end{bmatrix} . \tag{2.35}$$

The parameters appearing in the expression should be self-consistently determined. For example, we have

$$\frac{2-n}{n}=\langle rr^\dagger\rangle=\frac{\Omega}{(2\pi)^2}\int d^2k\,d\omega[1-f_F(\omega)]\left[-\frac{1}{\pi}\right]\mathrm{Im}S_{rr}(\omega,\mathbf{k}) \ , \tag{2.36}$$

where Ω is the volume of the unit cell and the integration is for the first Brillouin zone. We solve the above equations self-consistently in the next section.

As will be seen in the next section, the above approximation reproduces the single-CuO_2-cluster electronic excitation scheme quite well for the wide parameter range of the ratio t/Δ with $\Delta=\varepsilon_\eta-\varepsilon_p$. The weight arising from the residual interaction in Eq. (2.29) is estimated by evaluating the anticommutator according to the sum rule (A13). Rough estimations show that, except for $r_{\gamma_1}n_i$, the intersite contributions to the self-energy are of t_nb^3 order. The operator $r_{\gamma_1}n_i$ gives the t_nb-order correction to $m_P(\mathbf{k})$ near the Fermi level. However, it may be more suitable to treat this operator as a perturbation, since it is composed of operators in different sites and may show the energy behavior of a two-excitation continuum rather than an additional independent energy mode. Leaving a detailed treatment of residual terms to a future work, we make a rough estimation of the effect of the $r_{\gamma_1}n_i$ term to

$m_P(\mathbf{k})$ near the Fermi level in the t_n^2/Δ order and see how p-dominant bands are affected. Let us define an orthogonalized operator R as

$$R = r_s - b_{r_s} r - c_{r_s} P - d_{r_s} \Phi \ , \tag{2.37}$$

where

$$r_s = \sigma r_{\gamma_1} \mathbf{n} \ , \tag{2.38}$$

and the coefficients b_{r_s}, c_{r_s}, and d_{r_s} are chosen to satisfy

$$\langle \{R, r^\dagger\} \rangle = \langle \{R, P^\dagger\} \rangle = \langle \{R, \Phi^\dagger\} \rangle = 0 \ . \tag{2.39}$$

For the present purpose, we approximate the dynamical correction in Eq. (A11) for the P component as

$$\delta m_{PP}(\omega, \mathbf{k}) \approx \mathcal{F} t_n^2 \langle R R(x) R^\dagger(y) \rangle_I$$
$$\approx -t_n^2 \frac{I_R(\mathbf{k})}{\Delta} \ , \tag{2.40}$$

where

$$I_R(\mathbf{k}) = \mathcal{F} \langle \{R(\mathbf{x}), R^\dagger(\mathbf{y})\} \rangle \ . \tag{2.41}$$

Note that the energy shift (2.40) is a bit overestimated. Explicit forms of the coefficients b_{r_s}, c_{r_s}, and d_{r_s}, and normalization I_R are presented in Appendix B. Now the present approximation is valid up to $t_n b$ order, including intersite effects, as far as the p-dominant bands are concerned. The dynamical correction starts from $t_n b^3$ order.

III. RESULTS

By use of the formula in Sec. II and Appendix B, we calculate the spectral intensity of the p electron, $\sigma_{pp}(\omega)$, and the d electron, $\sigma_{\eta\eta}(\omega)$,

$$\sigma_{pp}(\omega) = \frac{\Omega}{(2\pi)^2} \int d^2k \left[-\frac{1}{\pi} \right] \mathrm{Im} S_{pp}(\omega, \mathbf{k}) \ , \tag{3.1}$$

$$\sigma_{\eta\eta}(\omega) = \frac{\Omega}{(2\pi)^2} \int d^2k \left[-\frac{1}{\pi} \right] \mathrm{Im} \frac{n}{2} S_{rr}(\omega, \mathbf{k}) \ , \tag{3.2}$$

where $S_{pp}(\omega, \mathbf{k})$ and $S_{rr}(\omega, \mathbf{k})$ are the retarded functions of p and r [$=(\sqrt{2/n})\eta$] operators, respectively.

First, in order to check the validity of the approximation, we show the comparison with the single-site result. We consider the case of the temperature $T=0$ K. When we switch off the intersite interaction (i.e., $\gamma_1=0$ in the formula in Sec. II and Appendix B), we should have a single-site result, which will be compared with the exact result presented in Appendix C. In Fig. 1 we show the energy levels and spectral intensity of one-particle excitations. The solid symbols indicate the calculated results in the present approximation, and the open symbols indicate the exact results. Δ is $\varepsilon_\eta - \varepsilon_p$; N is the total electron number per site in the ground state. Figure 1(a) is for $N=3$, and Fig. 1(b) is for $N=2$. Parameters are chosen for one hole to occupy mainly the Cu site in the $N=3$ ground state. The circles are for p-electron components, and the triangles are for d-electron components. The

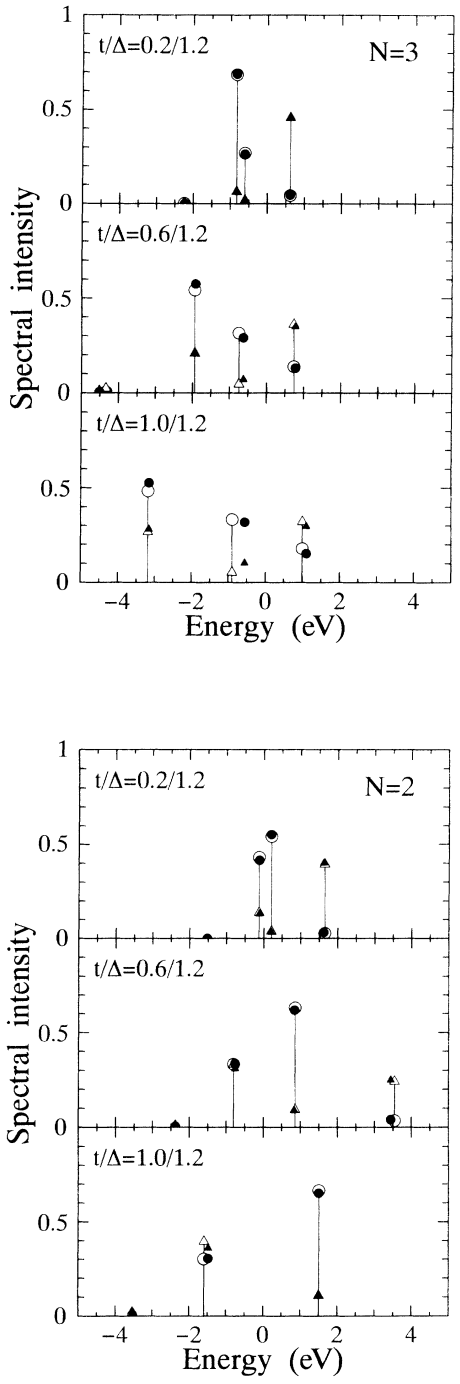

FIG. 1. (a) Spectral intensities for p and d electrons in the single-site case with $N=3$. Solid circles and triangles indicate p- and d-electron spectral intensities calculated in the present approximation, while open circles and triangles indicate corresponding exact results. Temperature T is 10^{-10} eV, and ε_p is chosen for the Fermi level ($\omega=0$) to be situated in the middle of the first and second lines. (b) Spectral intensities for p and d electrons in the single-site case with $N=2$. Solid circles and triangles indicate p- and d-electron spectral intensities calculated in the present approximation, while open circles and triangles indicate corresponding exact results. Temperature T is 10^{-10} eV, and ε_p is chosen for the Fermi level ($\omega=0$) to be situated in the middle of the first and second lines.

zero point of the energy is chosen at the Fermi level, so that the lines with $\omega>0$ show the transitions from N to $N+1$ and lines with $\omega<0$ show the transitions from N to $N-1$. From the figure we can see that the formulas in Sec. II reproduce the result of electronic excitations in the single site quite well for different electron numbers and a large range of the ratio t/Δ. Only for $N=3$ with large t/Δ ($=1.0/1.2$) [Fig. 1(a)] does the line just below the Fermi level show a slight deviation between the approximate and exact results. There are several quantities to determine mean fields as are shown in Appendix B. Important quantities are d-electron density n ($=\langle d^{\dagger}\cdot d\rangle$), p-hole density in the CuO_2 cluster $2a$ ($=2\langle p_\gamma p_\gamma^{\dagger}\rangle$), p-d mixing parameter b ($=\langle p_\gamma r^{\dagger}\rangle$), and p-hole–d-spin correlation parameter a_s ($=\langle p_\gamma p_\gamma^{\dagger}\sigma\cdot\mathbf{n}\rangle$). In Table I the calculated values for those parameters in the case of Fig. 1 are presented. n, n_p, and a change according to the rate of electron distribution induced by the p-d mixing. b shows the rate of p-d mixing, and it is proportional to t_n/Δ for small t_n/Δ and saturates for larger t_n/Δ,

$$b=\begin{cases}\dfrac{\lambda}{\sqrt{2(1+\lambda^2)(1+2\lambda^2)}} & \text{for } N=3\ ,\\ \dfrac{\nu}{\sqrt{(1+\nu^2)(1+2\nu^2)}} & \text{for } N=2\ ,\end{cases} \tag{3.3}$$

with

$$\lambda=\frac{2(2t)}{\Delta+\sqrt{\Delta^2+4(2t)^2}},\quad \nu=\frac{2\sqrt{2}(2t)}{\Delta+\sqrt{\Delta^2+8(2t)^2}}\ . \tag{3.4}$$

a_s changes largely with the change of N, which is because of the formation of the spin-singlet state

$$a_s=\begin{cases}0 & \text{for } N=3\ ,\\ \dfrac{3}{2(1+\nu^2)} & \text{for } N=2\ .\end{cases} \tag{3.5}$$

There are four lines in the spectral intensities. The lowest line is Φ dominant, but its intensity in p- and d-electron components is very small. In the $N=3$ case, the two lines below the Fermi level ($\omega=0$) are transitions to the singlet (closer line to the Fermi level) and triplet states from the ground state, respectively. The ratio of the intensity R in $\sigma_{pp}(\omega)$ is given by (see Appendix C)

$$R_{\text{singlet}}/R_{\text{triplet}}=\frac{(1+\sqrt{2}\lambda\nu)^2}{3(1+\nu^2)}\ , \tag{3.6}$$

so that it changes from $\frac{1}{3}$ to $\frac{1}{2}+\frac{1}{3}\sqrt{2}$ as t/Δ increases. The change of the above ratio is due to covalency; the singlet state is not purely composed of $n_p=1$ and $n_d=1$ states, and as t/Δ increases, the mixture of the singlet state with $n_d=2$ increases. In the approximate calculations, when Φ is neglected, the two lines below the Fermi level are very much modified: for small t/Δ, the position of the two lines is interchanged and, for large t/Δ, the level distance is narrowed and the intensity is transferred in a higher-energy line. This confirms that the inclusion of Φ is important to have the correct intensity distribution, although its intensity in p- and d-electron spectral intensities is small. The ground state of $N=2$ is the singlet state (here again we note that this singlet state is not purely composed of $n_p=1$ and $n_d=1$ states). Therefore the line just above the Fermi level in $N=2$ and the line just below the Fermi level in $N=3$ are of the same transition property. The change of weight for each line with hole doping is as follows. The reduction of the weight of the upper Hubbard level with hole doping becomes large with increasing t/Δ. The reduced ratio of p-electron intensity is (see Appendix C)

$$R^p_{N=2}/R^p_{N=3}=\frac{(\lambda-\sqrt{2}\nu)^2}{\lambda^2(1+\nu^2)}\ , \tag{3.7}$$

and the reduced ratio of d electron intensity is

$$R^d_{N=2}/R^d_{N=3}=\frac{1}{1+\nu^2}\ . \tag{3.8}$$

The presence of a p hole reduces the mixture of the p component to the upper Hubbard level. The singlet line in the spectral intensity increases largely when N is changed from 3 to 2. Such an increase occurs in the p-electron component. The reduction of the d-electron component in the upper Hubbard level is supplemented by the increase of the d-electron component in the triplet line.

Let us now present the results with intersite effects. First we show the results by putting $\delta m_{PP}=0$. Note that δm_{PP} shifts the energy position of the P component in the order of t_n^2/Δ, but as the effect to the p and r retarded functions, its contribution is one order reduced due to the mixing scheme. In the present approximation, the momentum dependence comes through $\gamma_1(\mathbf{k})$,

$$\gamma_1(\mathbf{k})=-\tfrac{1}{2}(\cos k_x a+\cos k_y a)\ . \tag{3.9}$$

The momentum integration is performed as

$$\int dx\frac{\Omega}{(2\pi)^2}\int d^2k\,\delta(x+\gamma_1(\mathbf{k}))=\int_{-1}^{1}dx\,w(x)\ . \tag{3.10}$$

For simplicity, we approximate

TABLE I. Calculated parameters in the single-site case.

$N=3$			
t/Δ	0.2/1.2	0.6/1.2	1.0/1.2
n	1.086	1.299	1.405
n_p	1.907	1.739	1.693
a	0.045 37	0.1299	0.1527
b	0.1866	0.2624	0.2529
a_s	−0.000 333 2	−0.021 25	−0.041 09
$N=2$			
t/Δ	0.2/1.2	0.6/1.2	1.0/1.2
n	1.129	1.325	1.388
n_p	0.8281	0.6810	0.6224
a	0.5849	0.6586	0.6880
b	0.2993	0.4028	0.4121
a_s	1.202	0.9762	0.8881

$$w(x)\approx\frac{1}{2}\ , \tag{3.11}$$

which corresponds to the approximation of Ref. 22,

$$\gamma_1(\mathbf{k})\approx\frac{\Omega}{2\pi}k^2-\frac{2\pi}{\Omega}\ . \tag{3.12}$$

The resulting bands are now approximately understood as ones created by mixing among the levels presented in Fig. 1. Although we start from operators defined in CuO_2 clusters, we can express overlapping of singlet and triplet excitations among different sites as well as mixing, since we treat not states restricted on CuO_2 clusters but operators expressing excitations. The mean fields induce intersite hopping and represent overlapping of those excitations. Level positions and weights are changed by the effects of the surrounding sites. There are important quantities to determine the electronic state in addition to the quantities n $(=\langle d^\dagger\cdot d\rangle)$, $2a$ $(=2\langle p_\gamma p_\gamma^\dagger\rangle)$, b $(=\langle p_\gamma r^\dagger\rangle)$, and a_s $(=\langle p_\gamma p_\gamma^\dagger\sigma\cdot\mathbf{n}\rangle)$. They are the nearest-neighbor spin correlations χ_s' $(=\frac{1}{3}\langle\mathbf{n}\cdot\mathbf{n}'\rangle)$ and χ_{ds}' $(=\frac{1}{3}\langle\mathbf{n}'\cdot p_\gamma^\dagger\sigma r\rangle)$, where the prime indicates the nearest-neighbor quantities. The mean fields χ_s' and χ_{ds}' are not calculable from the self-consistency of fermion propagators only. These nearest-neighbor spin correlations give a restriction on electron hopping from the spin freedom. In this paper we treat χ_s' and χ_{ds}' as parameters given by hand to clarify their roles.

First we give the result in which $\chi_s'=\chi_{ds}'=0$. In this case the intersite hopping is induced only by p-r mixing, $t_n\gamma(\mathbf{k})$. The result for $t/\Delta=0.6/1.2$ is presented in Fig. 2. The fine solid lines indicate the p-electron density of states (DOS), and the bold solid lines are for the d-electron density of states. The present result in the mean-field approximation produces qualitatively the result of Ref. 22 with dynamical corrections; that is, with hole doping, the DOS of the p-dominant band near the Fermi level (let us call this band an A band) increases its p-electron component with reducing the p-electron component from the upper Hubbard band and also from the lower p-dominant band (let us call this band B band). Note that A and B bands are formed by the mixture of singlet and triplet excitations. The calculated parameters are given in Table II. In the table the dashed quantities relate to the nearest-neighbor expectation values $a'=\langle p_\gamma p_\gamma^{\dagger\prime}\rangle$, $b'=\langle p_\gamma r^{\dagger\prime}\rangle$, and $b_s'=\langle r' p_s^\dagger\rangle$. The d-electron number is little changed; therefore, d holes in the upper Hubbard band are transferred just above the Fermi level. Since Fig. 2 shows that in the same time the occupied d component of the A band is transferred to the B band, the net intensity transfer of the d component occurs from the upper Hubbard band to the B band. This analysis shows that the upper Hubbard band reduces its p-electron component with hole doping, while the change of its d-electron component with doping is small. This is consistent with the experiment of O $1s\rightarrow 2p$ edge x-ray absorption and Cu $2p\rightarrow 3d$ edge x-ray absorption.[39] By comparing Figs. 1 and 2, we note that the rate of intensity transfer among bands roughly follows the tendency of the single-site result, although the intersite effect accelerates the change. Note that the change of the hole number per CuO_2 cluster is 1 in Fig. 1, while it is ~ 0.2 in Fig. 2. In Fig. 3 we show the spectral intensity of the single-site p-d model with finite U $(t/\Delta=0.6/1.2)$ for $N=3$ [Fig. 3(a)] and $N=2$ [Fig. 3(b)], where U is the on-site Coulomb repulsion on the Cu site. From this figure we can see that the reduction of the d component of the upper Hubbard band depends on the value of U. For $U\leq 5$, we must consider the effect of the lower Hubbard level. The discrepancy for the intensity transfer of the d component between the results of Fig. 2 and simulations[25,26] may be the difference of the value of U. Summarizing, holes are mostly doped in p-electron components and form a p-dominant band at the Fermi level; that is, p electrons circumvent the mixing with the upper Hubbard level and tunnel through by use of the bond excitation P.

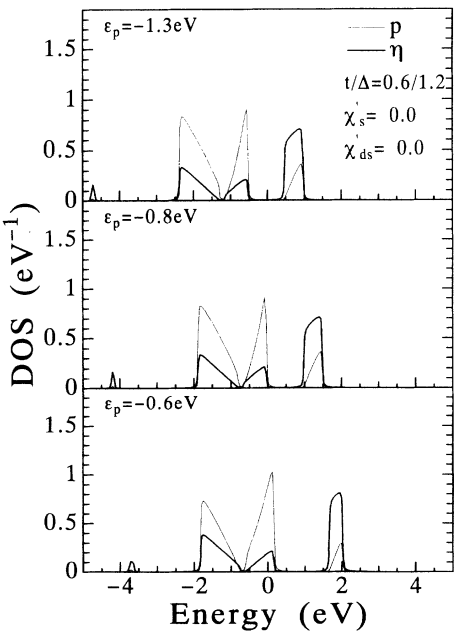

FIG. 2. Density of states for p and d electrons with $\chi_s'=\chi_{ds}'=0$.

Next we investigate effects of nearest-neighbor spin correlation. The local spin correlations χ_s' and χ_{ds}' have roughly the relation

$$\chi_{ds}'\approx 2b\chi_s'\ , \tag{3.13}$$

TABLE II. Calculated parameters with lattice effects for $\chi_s'=\chi_{ds}'=0$. Given parameters are $\Delta=1.2$ eV, $t=0.6$ eV, and $T=0.010$ eV.

ε_p	−1.30	−0.80	−0.60
n	1.313	1.313	1.334
n_p	1.763	1.754	1.519
$n_h=3-n-n_p$	−0.075	−0.067	0.147
a	0.1515	0.1580	0.3505
b	0.2486	0.2498	0.2939
a_s	−0.0256	−0.015 90	0.3215
a'	−0.0711	−0.0756	−0.1962
b'	−0.079 54	−0.0809	−0.1238
b_s'	−0.0336	−0.0369	−0.1335

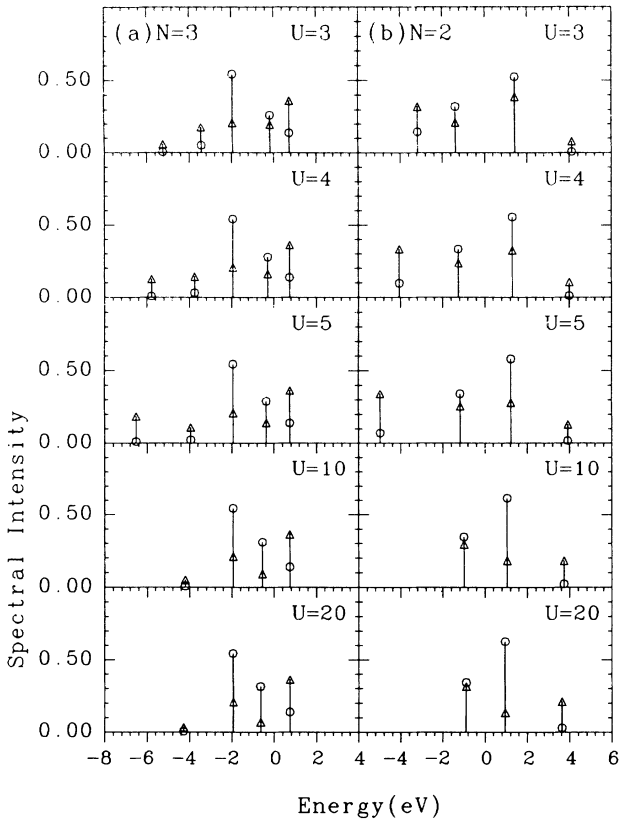

FIG. 3. Spectral intensities for p and d electrons in the single-site case with finite U and $t/\Delta=0.6/1.2$. Open circles are for p electrons, and open triangles are for d electrons. (a) is for $N=3$, and (b) is for $N=2$.

since

$$\langle n_i n'_{+i}\rangle \approx \langle n_i n'_i\rangle \langle n'_i n'_i\rangle^{-1}\langle n'_i n'_{+i}\rangle \ , \tag{3.14}$$

with $n_{+i}=p^{\dagger}_{\gamma}\sigma_i r$. The mean field χ'_s represents the nearest-neighbor spin correlation, and the range of the value is from $-1(2-n)$ (local singlet limit) to $\frac{1}{3}(2-n)$ (local triplet limit), where $(2-n)$ is the magnitude of the on-site spin χ_s $[=\frac{1}{3}\langle \mathbf{n}\cdot\mathbf{n}\rangle=(2-n)]$. In the antiferromagnetic limit, it has the value $-\frac{1}{3}(2-n)$. Note that χ'_s can be negative even though there is no long-range antiferromagnetic order; it shows only the nearest-neighbor spin order as average. With decreasing antiferromagnetic correlation, χ'_s approaches zero. In Fig. 4 we present the result with $\chi'_s=-0.2$. The calculated parameters are given in Table III. The on-site parameters a,b,a_s are not much different from the ones in Table II. The most prominent effect of the antiferromagnetic correlation is the change of the bandwidth. The upper Hubbard band is narrowed considerably. In the d-electron hopping, the spin configuration puts a strong restriction because of the Pauli principle. In the nearest-neighbor antiferromagnetic correlation, the spin flip is necessary for the nearest-neighbor hopping. Therefore the bandwidth should be reduced from $t_n b$ to the energy necessary for the spin flip, $t_n b^3$, where b is a p-d mixing parameter, $b=\langle p_{\gamma} r^{\dagger}\rangle$, and

TABLE III. Calculated parameters with lattice effects for $\chi'_s=-0.2$ and $\chi'_{ds}=2b\chi'_s$. Given parameters are $\Delta=1.2$ eV, $t=0.6$ eV, and $T=0.010$ eV.

ε_p	−1.40	−0.90	−0.60
n	1.328	1.326	1.336
n_p	1.760	1.755	1.500
$n_h=3-n-n_p$	−0.088	−0.081	0.164
a	0.1609	0.1646	0.3593
b	0.2493	0.2506	0.3046
a_s	−0.007 843	−0.002 047	0.3489
a'	−0.082 87	−0.084 77	−0.1922
b'	−0.090 47	−0.091 13	−0.1291
b'_s	−0.090 58	−0.091 75	−0.1723

it is proportional to t/Δ for small t/Δ. The same effect can be seen at the top of the band just below the Fermi level (A band). This band is expected to be dominantly of singlet character, although the triplet character may be mixed, as can be seen from the single-site result. The result shows that, differently from the upper Hubbard band, this band has a bandwidth of the order $t_n b$ as total. In order to see the effect of the local spin correlation more closely, we present the band dispersion in the p-electron spectral function. In Fig. 5 we show the energy dispersion corresponding to the case of Fig. 4 with $\varepsilon_p=-0.9$ eV. We can see that the energy dispersion of the A band is flat in the zone boundary, while roughly from the half zone the energy dispersion extended over the range $t_n b$. We expected that the local antiferromagnetic correlation would work to narrow the bandwidth in the same way as in both the upper Hubbard and A bands by restricting the electron hopping from spin freedom. However, the obtained result shows quite different

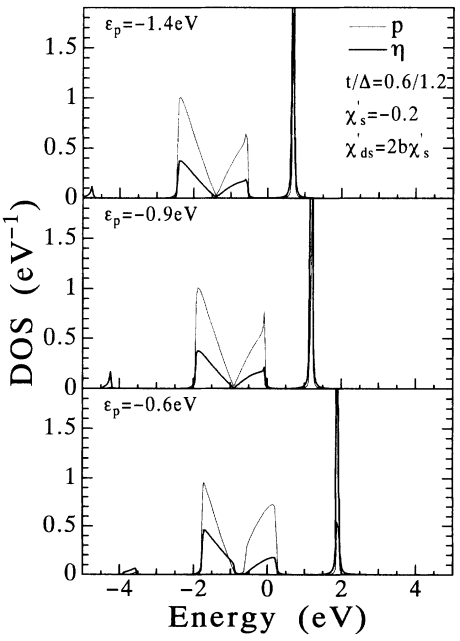

FIG. 4. Density of states for p and d electrons with $\chi'_s=-0.2$ and $\chi'_{ds}=2b\chi'_s$.

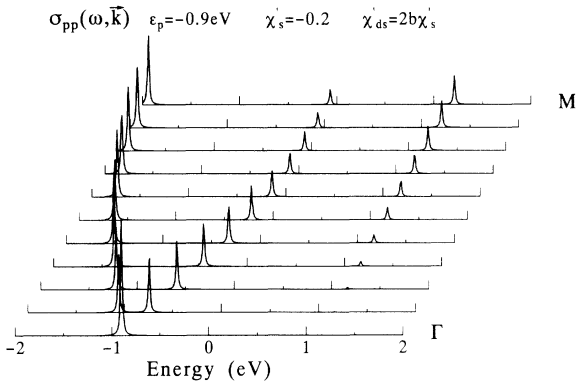

FIG. 5. Spectral density of p electrons $\sigma_{pp}(\omega,\mathbf{k})$ with $\chi'_s=-0.2$ and $\chi'_{ds}=2b\chi'_s$.

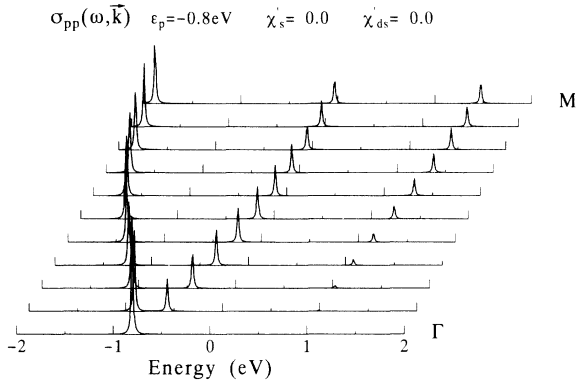

FIG. 6. Spectral density of p electrons $\sigma_{pp}(\omega,\mathbf{k})$ with $\chi'_s=\chi'_{ds}=0$.

behavior. The narrowing of the upper Hubbard band occurs as we expect. The A band receives its effect only around the zone boundary. The reason may be sought in the p-d coupling constant $t_n\gamma(\mathbf{k})$. The original of the p-d spin-spin interaction is the p-d mixing, and in the periodic array the mixing strength changes with momentum, especially at $\mathbf{k}=0$, $\gamma^2(\mathbf{0})=0$. Therefore at the zone center the A and B bands coincide at ε_p without mixing the d-electron component. This means that one cannot construct the A band only from the excitations to the spin-singlet states in the whole Brillouin zone. In the zone center, the excitations to the triplet states are largely mixed and therefore the restriction from the spin freedom may be weakened. The t-J model is derived by assuming the singlet formation of p holes and Cu spins in CuO_2 clusters. In the present case, the singlet formation in a single CuO_2 cluster is complete as is investigated in Fig. 1. Nevertheless, we have narrowing of the A band only from the zone boundary up to the middle of the zone. The overlapping of the CuO_2 clusters in the periodic array requires the equal coupling of a p electron to the neighboring d electrons, which produces the coupling $t_n\gamma(\mathbf{k})$. The different band structure of the present analysis from the one in the t-J model may originate from the different treatment of the overlapping of CuO_2 clusters; that is, in the present analysis, the momentum-dependent p-d mixing prevents the formation of the p-dominant band only from the singlet state in the whole Brillouin zone.

We present in Fig. 6 the energy dispersion for the case of Fig. 2 ($\chi'_s=\chi'_{ds}=0$) with $\varepsilon_p=-0.8$ eV just before the hole is doped. The band slope around the zone boundary is flatter in the case of Fig. 5 with $\chi'_s=-0.2$. Also the intensity in the band edge is reduced in Fig. 5. This can be understood as the effect of $I_P(\mathbf{k})$, i.e., $I_P(\mathbf{0})>I_P(\mathbf{Q})$ [$\mathbf{Q}=(\pi/a,\pi/a)$] for negative χ'_s. In the present approximation, the hole is doped by forming a small Fermi surface at the zone boundary and with hole doping it rapidly, forming a large Fermi surface. When we choose $\chi'_s=-\frac{1}{3}$, for example, the band dispersion is reversed near the middle of the zone as shown in Fig. 7. Negative larger χ'_s means the tendency to form local spin singlets. This also indicates that χ'_s is adjustable to form a flat dispersion from the middle of the zone to the zone boundary. With hole doping the antiferromagnetic correlation may be reduced; then, the band slope is rapidly recovered to the one with $\chi'_s=0$. Whether or not the Fermi surface is large at very small doping is not conclusive in the present approximation, although in the moderately doped region, the results with both $\chi'_s=0$ and $\chi'_s=-0.2$ are consistent with the large Fermi surface. In the four-site cluster simulation of the exact diagonalization with periodic boundary condition,[27] it is reported that the energy minima occur at the middle of the zone on the closest band to the Fermi level. In our calculation the intensity at the zone boundary in the A band is small, and the intensity in the upper Hubbard band is large at the zone boundary and it is small at the center of zone. This is also consistent with the result of the simulation.[27]

Finally, we show how the shift of the P level through δm_{PP} given in Eq. (2.40) modifies the A band. Figure 8 is for the DOS, and Fig. 9 is for the spectral function $\sigma_{pp}(\omega,\mathbf{k})$. The DOS of the A band is slightly narrowed, and the band edge is a bit rounded. From Fig. 9 one can see that the flat region of the A band is reduced, and this

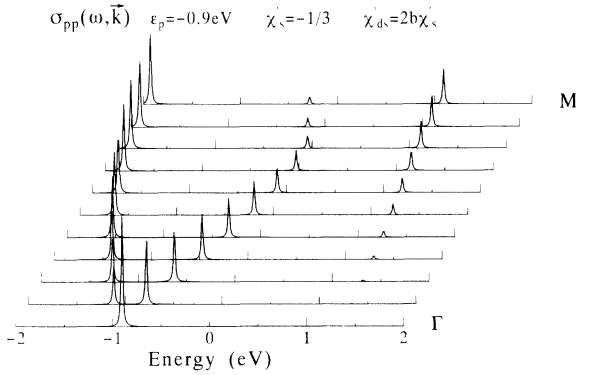

FIG. 7. Spectral density of p electrons $\sigma_{pp}(\omega,\mathbf{k})$ with $\chi'_s=-\frac{1}{3}$ with $\chi'_{ds}=2b\chi'_s$.

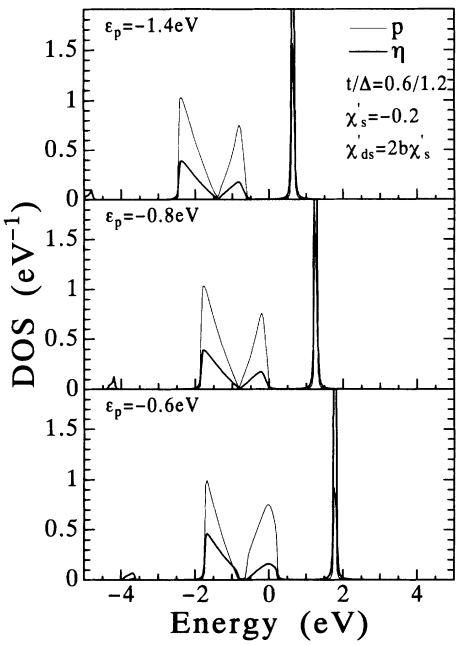

FIG. 8. Density of states for p and d electrons with $\chi_s'=-0.2$ and $\chi_{ds}'=2b\chi_s'$, including the correction δm_{PP} in Eq. (2.40).

is the origin of the rounding of the DOS. The above change is due to the momentum dependence of $\varepsilon_P(\mathbf{k})$, where

$$\varepsilon_P(\mathbf{k})=[m_P(\mathbf{k})+\delta m_{PP}(\mathbf{k})]I_P(\mathbf{k})^{-1} . \tag{3.15}$$

By expanding with respect to γ_1, we have

$$\begin{aligned}\varepsilon_P(\mathbf{k})\approx&(m_{P0}+\delta m_{PP0})(I_P^{-1})_0\\&+[m_{PP1}(I_P^{-1})_0+m_{PP0}(I_P^{-1})_1\\&+\delta m_{PP0}(I_P^{-1})_1]\gamma_1 ,\end{aligned} \tag{3.16}$$

where m_{PP0}, m_{PP1}, etc., are expansion coefficients. The coefficients in front of γ_1 produces a t_nb-order value, and δm_{PP0} works to reverse its slope. In the moderately

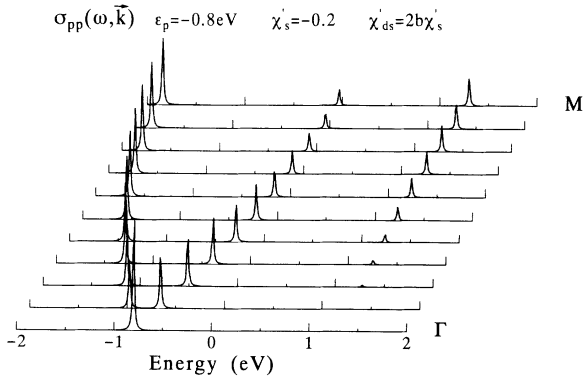

FIG. 9. Spectral density of p electrons $\sigma_{pp}(\omega,\mathbf{k})$ with $\chi_s'=-0.2$ and $\chi_{ds}'=2b\chi_s'$ for the case of Fig. 8.

doped region, the Fermi surface is consistent with a large Fermi surface. This analysis shows that the modification occurs in a small energy region ($\sim t_nb^3$) near the Fermi level. To discuss further the behavior of the band near the Fermi level, we must include the t_nb^3-order correction and also calculate χ_s', which is beyond the present approximation.

IV. CONCLUDING REMARKS

In this paper we have investigated the highly correlated p-d model in the mean-field approximation and studied in detail factors which change the distribution of the density of states with hole doping. Electronic excitations are described as a combination of composite electronic excitations in the CuO_2 cluster. The mean fields are defined for those composite excitations, and they describe the level shifts and hopping matrices among those excitations in the lattice. It is pointed out that the order of the approximation is determined by the weight of the operators. By identifying the basis of the composite operators with a weight of order 1 in a CuO_2 cluster, we have chosen a series of operators which reproduce the single-site result. Then the bands are formed by mixing among those composite excitations.

The change of the density of states with hole doping in the mean-field approximation is summarized as follows. With hole doping, holes are mostly doped in the p-electron component and form a p-electron-dominant band at the Fermi level. The DOS of the p-dominant A band near the Fermi level increases its p-electron component with reducing the p-electron component from the upper Hubbard band and the lower p-dominant B band. In the $U=\infty$ model, a small part of the d-electron component in the upper Hubbard band is transferred to the lower B band, but in the upper Hubbard band the total intensity of the d component is little changed. Only the p component is transferred at the Fermi level. This is consistent with the experimental result of O $1s\rightarrow 2p$ edge absorption and Cu $2p\rightarrow 3d$ edge absorption.[39] This result gives us a picture that p electrons circumvent the mixing with the upper Hubbard level and tunnel through by use of the bond excitation P.

The bands are formed from the single-site excitation levels, the upper Hubbard level, spin-singlet excitation level, and spin-triplet excitation level. With hole doping, the p-d spin-correlation parameter a_s, changes rapidly, representing an increase of doped holes in the spin-singlet states. The bandwidth is primary determined by the p-d mixing parameters t and b ($=\langle p_\gamma r^\dagger\rangle$) as t_nb. However, the bandwidth is very much affected by the nearest-neighbor spin correlations χ_s' and χ_{ds}'. In the limit of the antiferromagnetic correlation, the upper Hubbard band is almost flat. In the p-dominant A band near the Fermi level, the zone boundary is strongly affected. The A band becomes flat in a certain region centered at the zone boundary. From the middle of the zone to the zone center, this band has a dispersion of order t_nb. In a moderately doped region, the hole doping occurs consistently to form a large Fermi surface. The rapid formation of the large Fermi surface may indicate a rapid satu-

ration of the plasma frequency with carrier doping, consistent with the experiment of optical conductivity.[9]

Since χ_s' is not calculable only within the present scheme of fermionic propagators, it is not conclusive whether or not a large Fermi surface is realized just at the metal-insulator transition from the present analysis. The doping dependence of the T-linear coefficient of the specific heat may be also related to this problem of large or small Fermi surface. Since the slope of the electron energy spectrum is controlled by χ_s', it is necessary to include the evaluation of spin fluctuations, which is beyond the present approximation. If the spin susceptibility of the Cu spin changes from a local behavior to an itinerant one with carrier doping, the local antiferromagnetic correlation χ_s' may be weakened , and a change of the energy slope is expected. The present analysis shows that the flattening of the band dispersion occurs within the energy range of tb^3 order. We point out that in the present self-consistent approximation a case with a small Fermi surface is also consistent with the Luttinger theorem by the appearance of zero points in the propagators.

In the present analysis, the dynamical correction is neglected. Therefore any pole that appears in the propagators is a stable one. The effect of the $r_{\gamma_1} n_i$ term with weight of order 1 is evaluated by a simple approximation. This term gives the shift of the P component in the $t_n b$ order. Therefore neglected dynamical corrections start from the $t_n b^3$ order. Such corrections may be treated as a perturbation to discuss low-energy behavior. By loop corrections we can include effects in which constituent modes, such as p electrons and spin fluctuation, behave independently. Mean fields describe the effects of local correlation, while loop corrections describe higher-order intersite corrections. When the self-energy correction through the antiferromagnetic spin fluctuation is considered, a continuum of electron and spin fluctuations may cover the present band structure with a half-zone-shifted structure, and near the Fermi level the electronic state may have a structure in which the stable band is formed from the zone boundary to the middle of the zone and the continuum composed of p electrons and antiferromagnetic spin fluctuations from the middle of the zone to the zone center with reducing intensity. This may affect the behavior of the electronic properties near the Fermi level. One indication of the importance of this correction is found in Ref. 22 where we have shown that the imaginary part of the self-energy of the electron increases its intensity very rapidly with departing from the Fermi level due to the effect of spin fluctuation, although it vanishes at $\omega=0$ with $T=0$ K. A self-consistent treatment of spin fluctuation and a study of the effect of the dynamical correction are in progress.

ACKNOWLEDGMENTS

The authors would like to thank for useful discussions Dr. T. Koyama and S. Takahashi. This work was supported by a Grant-in-Aid, Ministry of Education, Japan. One of us would like to express his thanks for the financial support of the Kasuya fund.

APPENDIX A: OPERATOR EXPANSION

In this appendix we briefly summarize the composite-operator method which was proposed in Ref. 22. In the composite-operator method, electronic excitations are represented as a combination of several composite electronic operators extended over several lattice points which express certain collective excitations. There are many causes by which such collective excitations are formed; for example, they may originate from the occupation number dependence of the electron energy arising from the intra-atomic Coulomb interaction, from a molecular structure relating to a covalent bonding, or from a bound state formed by certain interactions. How to identify a series of composite operators depends on the systems and their ground-state properties.

Let us assume that we have identified an appropriate series of fermionic operators $\psi_n(\mathbf{x})$. The time derivatives of them are expressed as an expansion in terms of this series of operators and residual terms,

$$i\frac{\partial}{\partial t}\psi_n(x)=\sum_{n'}\varepsilon_{nn'}(-i\nabla)\psi_{n'}(x)+\delta j_n(x)=j_n(x)\ , \tag{A1}$$

where x indicates $(t,\mathbf{x})$ and $\varepsilon_{nn'}(-i\nabla)$ indicates that the coefficients $\varepsilon_{nn'}$ operate as the momentum-dependent $\varepsilon_{nn'}(\mathbf{k})$ on the Fourier transform of $\psi_n(x)$. As the normalization of operators, we use the norm

$$I_{nl}(\mathbf{k})=\mathcal{F}\langle\{\psi_n(\mathbf{x}),\psi_l^\dagger(\mathbf{y})\}\rangle\ , \tag{A2}$$

where $\mathcal{F}$ indicates the Fourier transform and is defined for arbitrary function $f(\mathbf{x})$ as

$$\mathcal{F}f(\mathbf{x})=\int d^2x\, e^{-i\mathbf{k}\cdot\mathbf{x}}f(\mathbf{x})\ . \tag{A3}$$

The expansion coefficients are defined from

$$\begin{aligned} m_{nl}(\mathbf{k})&\equiv\sum_{l'}\varepsilon_{nl'}(\mathbf{k})I_{l'l}(\mathbf{k})\\ &=\mathcal{F}\langle\{j_n(\mathbf{x}),\psi_l^\dagger(\mathbf{y})\}\rangle\ , \end{aligned} \tag{A4}$$

with

$$\langle\{\delta j_n(\mathbf{x}),\psi_l^\dagger(\mathbf{y})\}\rangle=0\ . \tag{A5}$$

The coefficients $\varepsilon_{nl}(\mathbf{k})$ are mean fields which represent the level shift and on-site and intersite mixing among composite excitations. The matrix $m_{nl}(\mathbf{k})$ has the Hermiticity property

$$m_{nl}(\mathbf{k})=m_{ln}(\mathbf{k})^*\ , \tag{A6}$$

since

$$\left\langle\left\{i\frac{\partial}{\partial t}\psi_n(\mathbf{x}),\psi_l^\dagger(\mathbf{y})\right\}\right\rangle=\left\langle\left\{\psi_n(\mathbf{x}),-i\frac{\partial}{\partial t}\psi_l^\dagger(\mathbf{y})\right\}\right\rangle\ . \tag{A7}$$

Then the retarded function $\langle R\psi_n(x)\psi_l^\dagger(y)\rangle$ is obtained in the form

$$\mathcal{F}\langle R\psi_n(x)\psi_l^\dagger(y)\rangle=\left[\frac{1}{\omega-\varepsilon(\mathbf{k})-\Sigma(\omega,\mathbf{k})}I(\mathbf{k})\right]_{nl}\ , \tag{A8}$$

where $\mathcal{F}$ indicates the Fourier transform and is defined by

$$\mathcal{F}\langle R\psi_n(x)\psi_l^\dagger(0)\rangle = -i\int dt\, d^2x\, e^{i\omega t - i\mathbf{k}\cdot\mathbf{x}}\langle R\psi_n(x)\psi_l^\dagger(0)\rangle \ . \quad \text{(A9)}$$

The self-energy $\Sigma(\omega,\mathbf{k})$ and $\Sigma^\dagger(\omega,\mathbf{k})$ are defined by

$$\langle R\delta j_n(x)\psi_l^\dagger(y)\rangle = \sum_{n'}\Sigma_{nn'}\left[i\frac{\partial}{\partial t_x}, -i\nabla_x\right]\langle R\psi_{n'}(x)\psi_l^\dagger(y)\rangle \quad \text{(A10a)}$$

and

$$\langle R\psi_n(x)\delta j_l^\dagger(y)\rangle = \sum_{l'}\Sigma_{l'l}^\dagger\left[-i\frac{\partial}{\partial t_y}, i\nabla_y\right]\langle R\psi_n(x)\psi_{l'}^\dagger(y)\rangle \ . \quad \text{(A10b)}$$

They are obtained from

$$\delta m_{nl}(\omega,\mathbf{k}) \equiv \mathcal{F}\langle R\delta j_n \delta j_l^\dagger\rangle_I = \Sigma(\omega,\mathbf{k})I(\mathbf{k}) = I(\mathbf{k})\Sigma^\dagger(\omega,\mathbf{k}) \ , \quad \text{(A11)}$$

where the subscript I indicates the irreducible part and, from Eqs. (A8) and (A10), is defined by

$$\langle R\delta j_n(x)\delta j_l^\dagger(y)\rangle_I = \langle R\delta j_n(x)\delta j_l^\dagger(y)\rangle - \sum_{l'}\Sigma_{l'l}^\dagger\left[-i\frac{\partial}{\partial t_y}, i\nabla_y\right]\langle R\delta j_n(x)\psi_{l'}^\dagger(y)\rangle \ . \quad \text{(A12)}$$

The dynamical correction $\delta m(\omega,\mathbf{k})$ satisfies the sum rule

$$\int d\omega\left[-\frac{1}{\pi}\right]\mathrm{Im}\delta m_{nl}(\omega,\mathbf{k}) = \mathcal{F}\langle\{\delta j_n(\mathbf{x}),\delta j_l^\dagger(\mathbf{y})\}\rangle \ . \quad \text{(A13)}$$

The residual term $\delta j_n(x)$ is usually expressed as a sum of certain operator products multiplied by coupling constants. Then the sum rule (A13) shows that the order of the correction is estimated from the order of the coupling constants multiplied by the norm of the concerned operators. Since the residual terms are expressed as higher-order operator products, whose contributions arise from multiparticle states, higher-order operator products may have smaller weights after orthogonalization. It should be noted that the choice of the series depends in general on the property of the ground state, and therefore the weight $I_{nl}(\mathbf{k})$ varies as the ground state is modified. Since the order of the approximation is determined not only by the coupling constants but also by the weight of the residual operators, the present scheme gives a kind of self-consistent perturbation scheme without depending on the magnitude of the coupling constants. Applicability of the approximation depends on how one properly chooses the basis operators to express excitations, which covers a wide range of parameters. It should be noted that the expression (A8) is exactly same as the one obtained from the projection operator method.[40,41,23,24]

As for $\psi_n(x)$, we choose simple operator products of fundamental fields which appear in the equation of motion. When a certain bound state if formed, extending over several lattice points, a proper operator to express this bound state must be chosen. In the p-d model of oxide superconductors, we expect the excitations to be primarily local, since the system is close to the ionic crystal. Then the natural candidates of a series $\psi_n(x)$ are electronic excitations in a CuO_2 cluster (or an extended cluster if necessary).

APPENDIX B: EXPLICIT FORMS OF I AND m

In this appendix we present the explicit forms of the normalization matrix I_{nl} and the mean field m_{nl}. We first sketch the procedure of the calculation of them.

We have

$$I_P = \langle\{P,P^\dagger\}\rangle = 3I_{ss} - 9b^2 \ , \quad \text{(B1)}$$

with

$$I_{ss} = \tfrac{1}{3}\langle\{p_s,p_s^\dagger\}\rangle \ , \quad \text{(B2)}$$

$$b = \langle p_\gamma r^\dagger\rangle \ , \quad \text{(B3)}$$

and

$$I_\Phi = \langle\{\Phi,\Phi^\dagger\}\rangle = I_{\varphi\varphi} - c_\phi^2 I_P \ , \quad \text{(B4)}$$

where

$$I_{\varphi\varphi} = \langle\{\varphi,\varphi^\dagger\}\rangle \ , \quad \text{(B5)}$$

with

$$\varphi = \phi - bp_\gamma \quad \text{(B6)}$$

and

$$c_\phi = \langle\{\phi,P^\dagger\}\rangle(I_P)^{-1} = 3I_{\phi s}I_P^{-1} \ , \quad \text{(B7)}$$

with

$$I_{\phi s} = \tfrac{1}{3}\langle\{\phi,p_s^\dagger\}\rangle \ . \quad \text{(B8)}$$

Therefore the calculation of I_P and I_Φ is reduced to the evaluation of the anticommutators I_{ss}, $I_{\varphi\varphi}$, and $I_{\phi s}$.

For an arbitrary operator A, we define the expansion in terms of ψ_n as

$$A = a_A p_\gamma + b_A r + c_A P + d_A\Phi + \delta A \ , \quad \text{(B9)}$$

where the coefficients are determined from Eq. (2.31). For example, we have the expansion

$$p_i(\equiv p_\gamma n_i) = b\sigma_i r + c_s\sigma_i P + \delta p_i \ , \quad \text{(B10a)}$$

$$p_0(\equiv p_\gamma\delta n) = br + c_0 P + d_0\Phi + \delta p_0 \ , \quad \text{(B10b)}$$

$$\phi = bp_\gamma + c_\phi P + \Phi \ , \quad \text{(B11)}$$

and

$$h_s = a_{hs}p_\gamma + b_{hs}r + c_{hs}P + d_{hs}\Phi + \delta h_s \ , \quad \text{(B12)}$$

$$\psi = a_\psi p_\gamma + b_\psi r + c_\psi P + d_\psi\Phi + \delta\Phi \ . \quad \text{(B13)}$$

Then c and d in m of Eq. (2.23) are expressed by c_s, c_0, and d_0, respectively. The mean fields m_P, $m_{P\Phi}$, and m_Φ are calculated by considering the Hermiticity condition

for m in Eq. (A6). The Hermiticity is taken with respect to the simple operator product of fundamental fields, and therefore the mean fields are calculated in such a way that the time derivative operates always to the lower-order operator product; that is, we use

$$m_P=\left\langle\left\{i\frac{\partial}{\partial t}P,P^\dagger\right\}\right\rangle$$
$$=\left\langle\left\{i\frac{\partial}{\partial t}p_s,p_s^\dagger\right\}\right\rangle-3b\left\langle\left\{i\frac{\partial}{\partial t}r,P^\dagger\right\}\right\rangle$$
$$-3b\left\langle\left\{P,-i\frac{\partial}{\partial t}r^\dagger\right\}\right\rangle-9b^2\left\langle\left\{i\frac{\partial}{\partial t}r,r^\dagger\right\}\right\rangle , \tag{B14}$$

$$m_{P\Phi}=\left\langle\left\{i\frac{\partial}{\partial t}P,\Phi^\dagger\right\}\right\rangle$$
$$=\left\langle\left\{i\frac{\partial}{\partial t}P,\phi^\dagger\right\}\right\rangle-m_Pc_\phi , \tag{B15}$$

and

$$m_\Phi=\left\langle\left\{i\frac{\partial}{\partial t}\Phi,\Phi^\dagger\right\}\right\rangle$$
$$=\left\langle\left\{i\frac{\partial}{\partial t}\phi,\phi^\dagger\right\}\right\rangle-(b^2\varepsilon_p\gamma^2+c_\phi^2m_P+2c_\phi m_{P\Phi}) . \tag{B16}$$

Evaluating the anticommutators for various composite operators, we have the normalization matrix I_{nm} in the form

$$I=\begin{bmatrix}1&0&0&0\\0&1&0&0\\0&0&I_P&0\\0&0&0&I_\Phi\end{bmatrix} , \tag{B17}$$

where

$$I_P=3I_{ss}-9b^2 , \tag{B18}$$
$$I_\Phi=I_{\varphi\varphi}-c_\phi^2I_P , \tag{B19}$$
$$c_\phi=3I_{\phi s}I_P^{-1} , \tag{B20}$$

and

$$I_{ss}=\tfrac{4}{3}a_s+\chi_s+\chi_s'\gamma_1 , \tag{B21}$$
$$I_{\phi s}\approx ab+\tfrac{1}{2}\chi_{ds}'\gamma_1 , \tag{B22}$$
$$I_{\varphi\varphi}\approx\frac{2-n}{n}(1-2a)+a^2-b^2$$
$$+\frac{2}{n}a_0(1+a)-a_r'\left[2a_r'+\frac{1}{4}\right]\gamma_1 . \tag{B23}$$

Here we used the notation

$$a=\langle p_\gamma p_\gamma^\dagger\rangle,\quad a_r'=\langle r'r^\dagger\rangle , \tag{B24}$$

with the prime indicating the nearest-neighbor lattice point,

$$a_s=\langle p_\gamma p_s^\dagger\rangle,\quad a_0=\langle p_\gamma p_0^\dagger\rangle , \tag{B25}$$
$$b=\langle p_\gamma r^\dagger\rangle , \tag{B26}$$
$$\chi_s=\tfrac{1}{3}\langle\mathbf{n}\cdot\mathbf{n}\rangle=2-n , \tag{B27}$$
$$\chi_s'=\tfrac{1}{3}\langle\mathbf{n}\cdot\mathbf{n}'\rangle , \tag{B28}$$
$$\chi_{ds}'=\tfrac{1}{3}\langle(p_\gamma^\dagger\boldsymbol{\sigma}r)\mathbf{n}'\rangle . \tag{B29}$$

The mean field is obtained in the form

$$m=\begin{bmatrix}\varepsilon_p&t_n\gamma(\mathbf{k})&0&0\\t_n\gamma(\mathbf{k})&\varepsilon_r&-\frac{t_n}{n}cI_P&-\frac{t_n}{n}dI_\Phi\\0&-\frac{t_n}{n}cI_P&m_P&m_{P\Phi}\\0&-\frac{t_n}{n}dI_\Phi&m_{\Phi P}&m_\Phi\end{bmatrix} , \tag{B30}$$

where

$$t_n=2t\sqrt{n/2} , \tag{B31}$$
$$\varepsilon_r=\varepsilon_\eta-2\frac{t_n}{n}b , \tag{B32}$$
$$c=3c_s-c_0 , \tag{B33}$$
$$d=-d_0 , \tag{B34}$$

with

$$c_s=\tfrac{1}{3},\quad c_0=-3b^2I_P^{-1} , \tag{B35}$$
$$d_0=(I_{\phi0}-c_\phi c_0I_P)I_\Phi^{-1} , \tag{B36}$$
$$I_{\phi0}\approx-ab+(2-n)b , \tag{B37}$$

and

$$m_P=\left[\varepsilon_p+3t_n\left[c_\phi+c_{hs}+\frac{2}{n}bc\right]\right]I_P$$
$$+9b[(\varepsilon_p-\varepsilon_r)b+t_nb_{h_s}] , \tag{B38}$$

$$m_{P\Phi}=3t_n\left[1+3d_{hs}+\frac{1}{n}bd\right]I_\Phi-3\frac{t_n}{n}bcc_\phi I_P$$
$$-9b[(\varepsilon_p-\varepsilon_r)b+t_nb_{hs}] , \tag{B39}$$

$$m_\Phi=\left[2\varepsilon_p-\varepsilon_\eta-2\frac{t_n}{n}d_0+t_nd_\psi\right]I_\Phi$$
$$+\left[-2\frac{t_n}{n}c_0+(2\varepsilon_p-\varepsilon_\eta)c_\phi+t_nc_\psi\right]c_\phi I_P$$
$$+b\left[-2t_n\frac{n-1}{n}+(\varepsilon_p-\varepsilon_\eta)b+t_na_\psi\right]\gamma^2$$
$$-c_\phi^2m_P-2c_\phi m_{P\Phi} . \tag{B40}$$

The necessary coefficients are calculated as

$$a_{hs}=0\ , \tag{B41a}$$

$$b_{hs}=-a-a_r'-\frac{1}{n}\left[\frac{1}{3}a_s+a_0\right]-\frac{1}{n}\chi_s'\gamma_1\ , \tag{B41b}$$

$$c_{hs}=-[\tfrac{4}{3}b_s'+2b(1-a)+3ab+3bb_{hs}+\tfrac{1}{2}\chi_{ds}'\gamma_1]I_P^{-1}\ , \tag{B41c}$$

$$d_{hs}=(-bb'+b'^2\gamma_1-c_\phi c_{hs}I_P)I_\Phi^{-1}\ , \tag{B41d}$$

$$a_\psi=1-a-a_r'+\frac{1}{n}(a_s-a_0)\ , \tag{B42a}$$

$$d_\psi I_\Phi+c_\psi c_\phi I_P=\langle\{\psi,\varphi^\dagger\}\rangle=\frac{1}{n}(1-a)d_0I_\Phi+\frac{1}{n}(1-a)(c_0+3c_s)c_\phi I_P+I_{:\psi:\varphi}\ , \tag{B42b}$$

with

$$I_{:\psi:\varphi}=\langle\{:\psi:,\varphi^\dagger\}\rangle \approx 2\left[\frac{2-n}{n}-a\right]b'-\frac{2}{n}(b_0'+a_0b'+ab_0')+\left\{-(1-2a)+a_r'+\frac{1}{n}[2a^2-(2-n)(1-2a)]-\frac{1}{n}(a_s-a_0)\right\}b + \left\{2a_r'b''+\left[2a'+\frac{1}{4}\right]b'+\frac{1}{n}\left[2a_0'b'+\left[2a'+\frac{1}{4}\right](b_0'-b_s')\right]\right\}\gamma_1\ . \tag{B43}$$

Here the following notation is used:

$$b'=\langle r'p_\gamma^\dagger\rangle,\quad b_s'=\langle r'p_s^\dagger\rangle,\quad b_0'=\langle r'p_0^\dagger\rangle\ , \tag{B44}$$

$$b''=\langle(r')'p_\gamma^\dagger\rangle\ , \tag{B45}$$

$$a'=\langle p_\gamma'p_\gamma^\dagger\rangle,\quad a_0'=\langle p_\gamma'p_0^\dagger\rangle\ . \tag{B46}$$

An effect from a residual interaction, $r_s(=\sigma r_{\gamma_1}\mathbf{n})$, is evaluated within the above mean-field approximation as follows. First define R satisfying

$$\langle\{R,p^\dagger\}\rangle=\langle\{R,r^\dagger\}\rangle=\langle\{R,P^\dagger\}\rangle=\langle\{R,\Phi^\dagger\}\rangle=0$$

as

$$R=r_s-b_{r_s}r-c_{r_s}P-d_{r_s}\Phi\ . \tag{B47}$$

We have

$$b_{r_s}=-3\left[a_r'+\frac{1}{n}\chi_s'\gamma_1\right]\ , \tag{B48a}$$

$$c_{r_s}I_P=-3(\tfrac{4}{3}b_s'-\tfrac{1}{2}\chi_{ds}'\gamma_1+bb_{r_s})\ , \tag{B48b}$$

$$d_{r_s}I_\Phi=-(3b'b+c_\phi c_{r_s}I_P)\ . \tag{B48c}$$

Then $I_R=\langle\{R,R^\dagger\}\rangle$ is given by

$$I_R=I_{r_sr_s}-b_{r_s}^2-c_{r_s}^2I_P-d_{r_s}^2I_\Phi \tag{B49}$$

and $I_{r_sr_s}$ is evaluated as

$$I_{r_sr_s}=\sigma_i\langle\{r_{\gamma_1}n_i,n_jr_{\gamma_1}^\dagger\}\rangle\sigma_j \approx\sigma_i\{\langle r_{\gamma_1}r_{\gamma_1}^\dagger\rangle\langle n_in_j\rangle+\langle r_{\gamma_1}^\dagger r_{\gamma_1}\rangle\langle n_jn_i\rangle\}\sigma_j \approx\tfrac{3}{4}\chi_s\ , \tag{B50}$$

where in the last step we take only the on-site contribution.

The approximation in this appendix is valid up to t_nb order and residual interactions induce a t_nb^3-order correction.

APPENDIX C: SINGLE-SITE p-d MODEL

In order to see the validity of the approximation, we investigate how much the present scheme reproduces the exact result of the single-site case. We consider the single-site p-d model with $U=\infty$ given by

$$H=\tfrac{1}{2}\varepsilon_\eta\eta^\dagger\eta+\varepsilon_pp^\dagger p+2t(\eta^\dagger p+p^\dagger\eta)\ . \tag{C1}$$

When we switch off the intersite interaction in the formula obtained in Sec. III (i.e., put $\gamma_1=0$), we have the single-site result. The retarded Green function of the Hamiltonian (C1) is obtained by obtaining the eigenvectors and evaluating the trace in the thermal average. The total electron number is denoted by N, $N=n+n_p$, where n is the d-electron number and n_p is the p-electron number. The bare gap is denoted Δ $(=\varepsilon_\eta-\varepsilon_p)$, and the chemical potential μ is included in the definition of ε_η and ε_p; that is, ε_p should be read as $\varepsilon_p-\mu$, for example. In the limit of temperature $T=0$, we have the following results.

(1) $N=3$ ground state. In this case we have

$$n=1+\frac{\lambda^2}{1+\lambda^2}\ , \tag{C2}$$

$$n_p=2-\frac{\lambda^2}{1+\lambda^2}\ , \tag{C3}$$

with

$$\lambda=\frac{2(2t)}{\Delta+\sqrt{\Delta^2+4(2t)^2}} . \tag{C4}$$

We have, for the propagators,

$$S_{pp}(\omega)=\frac{1}{2}\frac{\lambda^2}{1+\lambda^2}\frac{1}{\omega-\varepsilon_u} + \frac{1}{4}\frac{1}{1+\lambda^2}\left\{\frac{(1+\sqrt{2}\lambda\nu)^2}{1+\nu^2}\frac{1}{\omega-\varepsilon_s}+3\frac{1}{\omega-\varepsilon_t} + \frac{(\nu-\sqrt{2}\lambda)^2}{1+\nu^2}\frac{1}{\omega-\varepsilon_\phi}\right\} , \tag{C5}$$

$$S_{\eta\eta}(\omega)=\frac{1}{2}\frac{1}{1+\lambda^2}\frac{1}{\omega-\varepsilon_u} + \frac{1}{4}\frac{\lambda^2}{1+\lambda^2}\left\{\frac{1}{1+\nu^2}\frac{1}{\omega-\varepsilon_s}+3\frac{1}{\omega-\varepsilon_t} + \frac{\nu^2}{1+\nu^2}\frac{1}{\omega-\varepsilon_\phi}\right\} , \tag{C6}$$

where

$$\varepsilon_u=\varepsilon_p+\tfrac{1}{2}[\sqrt{\Delta^2+4(2t)^2}+\Delta] , \tag{C7a}$$

$$\varepsilon_s=\varepsilon_p+\tfrac{1}{2}[\sqrt{\Delta^2+8(2t)^2}-\sqrt{\Delta^2+4(2t)^2}] , \tag{C7b}$$

$$\varepsilon_t=\varepsilon_p-\tfrac{1}{2}[\sqrt{\Delta^2+4(2t)^2}-\Delta] , \tag{C7c}$$

$$\varepsilon_\phi=\varepsilon_p-\tfrac{1}{2}[\sqrt{\Delta^2+8(2t)^2}+\sqrt{\Delta^2+4(2t)^2}] , \tag{C7d}$$

and

$$\nu=\frac{2\sqrt{2}(2t)}{\Delta+\sqrt{\Delta^2+8(2t)^2}} . \tag{C8}$$

(2) $N=2$ ground state. In this case we have

$$n=1+\frac{\nu^2}{1+\nu^2} , \tag{C9}$$

$$n_p=1-\frac{\nu^2}{1+\nu^2} . \tag{C10}$$

We have, for the propagators,

$$S_{pp}(\omega)=\frac{1}{2}\frac{1}{1+\nu^2}\frac{(\lambda-\sqrt{2}\nu)^2}{1+\lambda^2}\frac{1}{\omega-\varepsilon'_u} + \frac{1}{2}\frac{1}{1+\nu^2}\left\{\frac{(1+\sqrt{2}\lambda\nu)^2}{1+\lambda^2}\frac{1}{\omega-\varepsilon_s}+\frac{1}{\omega-\varepsilon_n}\right\} , \tag{C11}$$

$$S_{\eta\eta}(\omega)=\frac{1}{2}\frac{1}{1+\nu^2}\frac{1}{1+\lambda^2}\frac{1}{\omega-\varepsilon'_u} + \frac{1}{2}\frac{1}{1+\nu^2}\frac{\lambda^2}{1+\lambda^2}\frac{1}{\omega-\varepsilon_s}+\frac{\nu^2}{1+\nu^2}\frac{1}{\omega-\varepsilon_n} , \tag{C12}$$

where

$$\varepsilon'_u=\varepsilon_p+\tfrac{1}{2}[\sqrt{\Delta^2+8(2t)^2}+\sqrt{\Delta^2+4(2t)^2}] , \tag{C13a}$$

$$\varepsilon_s=\varepsilon_p+\tfrac{1}{2}[\sqrt{\Delta^2+8(2t)^2}-\sqrt{\Delta^2+4(2t)^2}] , \tag{C13b}$$

$$\varepsilon_n=\varepsilon_p-\tfrac{1}{2}[\sqrt{\Delta^2+8(2t)^2}-\Delta] . \tag{C13c}$$

[1] A. Fujimori, E. Takayama-Muromachi, Y. Uchida, and B. Okai, Phys. Rev. B **35**, 8814 (1987).

[2] J. C. Fuggle, P. J. W. Weijs, R. Schoorl, G. A. Sawatzky, J. Fink, N. Nücker, P. J. Durham, and W. M. Temmerman, Phys. Rev. B **37**, 123 (1988).

[3] V. J. Emery, Phys. Rev. Lett. **58**, 2794 (1987).

[4] F. Mila, Phys. Rev. B **38**, 11 358 (1988).

[5] M. S. Hybertsen, M. Schlüter, and N. E. Christensen, Phys. Rev. B **39**, 9028 (1989).

[6] H. Romberg, M. Alexander, N. Nücker, P. Adelmann, and J. Fink, Phys. Rev. B **42**, 8768 (1990).

[7] C. T. Chen, F. Sette, Y. Ma, M. S. Hybertsen, E. B. Stechel, W. M. C. Foulkes, M. Schluter, S.-W. Cheong, A. S. Cooper, L. W. Rupp, Jr., B. Batlogg, Y. L. Soo, Z. H. Ming, A. Krol, and Y. H. Kao, Phys. Rev. Lett. **66**, 104 (1991).

[8] T. Takahashi, S. Suzuki, T. Kusunoki, S. Sato, H. Katayama-Yoshida, A. Yamanaka, F. Minami, and S. Takekawa, Physica C **185-189**, 1057 (1991).

[9] S. Uchida, T. Ido, H. Takagi, T. Arima, Y. Tokura, and S. Tajima, Phys. Rev. B **43**, 7942 (1991).

[10] H. Matsuyama, T. Takahashi, H. Katayama-Yoshida, T. Kashiwakura, Y. Okabe, S. Sato, N. Kosugi, A. Yagishita, K. Tanaka, H. Fujimoto, and H. Inokuchi, Physica C **160**, 567 (1989).

[11] A. Fujimori, Physica B **163**, 736 (1990).

[12] T. Watanabe, T. Takahashi, S. Suzuki, S. Sato, and H. Katayama-Yoshida, Phys. Rev. B **44**, 5316 (1991).

[13] T. Takahashi, H. Matsuyama, H. Katayama-Yoshida, Y. Okabe, S. Hosoya, K. Seki, H. Fujimoto, M. Sato, and H. Inokuchi, Phys. Rev. B **39**, 6636 (1989).

[14] R. Manzke, T. Buslaps, R. Claessen, M. Skibowski, and J. Fink, Physica C **162-164**, 1381 (1989).

[15] C. G. Olson, R. Liu, A.-B. Yang, D. W. Lynch, A. J. Arko, R. S. List, B. W. Veal, Y. C. Chang, P. Z. Jiang, and A. P. Paulikas, Science **245**, 731 (1989).

[16] J. C. Campuzano, G. Jennings, M. Faiz, L. Beaulaigue, B. W. Veal, J. Z. Liu, A. P. Paulikas, K. Vandervoort, H. Claus, R. S. List, A. J. Arko, and R. J. Bartlett, Phys. Rev. Lett. **64**, 2308 (1990).

[17] H. Matsumoto, M. Sasaki, and M. Tachiki, Solid State Commun. **71**, 829 (1989); Phys. Rev. B **43**, 10 247 (1991); **43**, 10 264 (1991).

[18] H. Jichu, T. Matsuura, and Y. Kuroda, J. Phys. Soc. Jpn. **58**, 4280 (1989); **59**, 2820 (1990).

[19] P. C. Pattnaik and D. M. Newns, Phys. Rev. B **41**, 880 (1990); D. M. Newns, P. C. Pattnaik, and C. C. Tsuei, *ibid.* **43**, 3075 (1991).

[20] C. A. R. Sá de Melo and S. Doniach, Phys. Rev. B **41**, 6633 (1990).

[21] K. Levin, Ju H. Kim, J. P. Lu, and Qimiao Si, Physica C **175**,

449 (1991).
[22]H. Matsumoto, M. Sasaki, S. Ishihara, and M. Tachiki, Phys. Rev. B **46**, 3009 (1992); M. Sasaki, H. Matsumoto, and M. Tachiki, *ibid.* **46**, 3022 (1992).
[23]K. W. Becker, W. Brenig, and P. Fulde, Z. Phys. B **81**, 165 (1990); P. Fulde, *Electron Correlations in Molecules and Solids* (Springer-Verlag, Berlin, 1991).
[24]A. J. Fedro, Yu Zhou, T. C. Leung, B. N. Harmon, and S. K. Sinha, Phys. Rev. B **46**, 14 785 (1992).
[25]J. Wagner, W. Hanke, and D. J. Scalapino, Phys. Rev. B **43**, 10 517 (1991).
[26]T. Tohyama and S. Maekawa, Physica C **191**, 193 (1992).
[27]Y. Ohta, K. Tsutsui, W. Koshibae, T. Shimozato, and S. Maekawa, Phys. Rev. B **46**, 14 022 (1992).
[28]J. R. Schrieffer, X.-G. Wen, and S.-C. Zhang, Phys. Rev. Lett. **60**, 944 (1988); A. Kampf and J. R. Schrieffer, Phys. Rev. B **41**, 6399 (1990); **42**, 7967 (1990).
[29]T. Moriya, Y. Takahashi, and K. Ueda, J. Phys. Soc. Jpn. **59**, 2905 (1990).
[30]F. C. Zhang and T. M. Rice, Phys. Rev. B **37**, 3759 (1988).
[31]J. Zaanen and A. M. Oleś, Phys. Rev. B **37**, 9423 (1988).
[32]H. B. Schüttler and A. J. Fedro, J. Appl. Phys. **63**, 4209 (1988).
[33]S. Ishihara, H. Matsumoto, and M. Tachiki, Phys. Rev. B **42**, 10 041 (1990).
[34]H. Kohno and K. Yamada, Prog. Theor. Phys. **85**, 13 (1991).
[35]P. W. Anderson, Science **235**, 1196 (1987); Physica C **185-189**, 11 (1991).
[36]N. Nagaosa and P. A. Lee, Phys. Rev. Lett. **64**, 2450 (1990).
[37]P. W. Anderson, Phys. Rev. Lett. **64**, 1839 (1990); **67**, 2092 (1991).
[38]C. M. Varma, P. B. Littlewood, S. Schmitt-Rink, E. Abrahams, and A. E. Ruckenstein, Phys. Rev. Lett. **63**, 1996 (1989); A. E. Ruckenstein and C. M. Varma, Physica C **185-189**, 134 (1991).
[39]C. T. Chen, L. H. Tjeng, J. Kwo, H. L. Kao, P. Rudolf, F. Sette, and R. M. Fleming, Phys. Rev. Lett. **68**, 2543 (1992).
[40]H. Mori, Prog. Theor. Phys. **33**, 423 (1965).
[41]R. Zwanzig, *Lectures in Theoretical Physics* (Interscience, New York, 1961), Vol. 3.